Reevaluation of mid-Pliocene North Atlantic sea surface temperatures

Marci M. Robinson,[1] Harry J. Dowsett,[1] Gary S. Dwyer,[2] and Kira T. Lawrence[3]

Received 10 February 2008; revised 1 April 2008; accepted 9 June 2008; published 15 August 2008.

[1] Multiproxy temperature estimation requires careful attention to biological, chemical, physical, temporal, and calibration differences of each proxy and paleothermometry method. We evaluated mid-Pliocene sea surface temperature (SST) estimates from multiple proxies at Deep Sea Drilling Project Holes 552A, 609B, 607, and 606, transecting the North Atlantic Drift. SST estimates derived from faunal assemblages, foraminifer Mg/Ca, and alkenone unsaturation indices showed strong agreement at Holes 552A, 607, and 606 once differences in calibration, depth, and seasonality were addressed. Abundant extinct species and/or an unrecognized productivity signal in the faunal assemblage at Hole 609B resulted in exaggerated faunal-based SST estimates but did not affect alkenone-derived or Mg/Ca–derived estimates. Multiproxy mid-Pliocene North Atlantic SST estimates corroborate previous studies documenting high-latitude mid-Pliocene warmth and refine previous faunal-based estimates affected by environmental factors other than temperature. Multiproxy investigations will aid SST estimation in high-latitude areas sensitive to climate change and currently underrepresented in SST reconstructions.

Citation: Robinson, M. M., H. J. Dowsett, G. S. Dwyer, and K. T. Lawrence (2008), Reevaluation of mid-Pliocene North Atlantic sea surface temperatures, *Paleoceanography*, *23*, PA3213, doi:10.1029/2008PA001608.

1. Introduction

[2] The mid-Pliocene is the most recent period of global warmth analogous to future warming predicted by climate models [*Dowsett and Robinson*, 2006; *Intergovernmental Panel on Climate Change*, 2001]. The Pliocene Research, Interpretation and Synoptic Mapping (PRISM) Project reconstructs global synoptic mid-Pliocene surface conditions [*Dowsett et al.*, 1999], and PRISM sea surface temperature (SST) reconstructions are the most comprehensive pre-Pleistocene data sets available for analysis of warmer-than-present climates and for future climate modeling experiments [*Chandler et al.*, 1994; *Molnar and Cane*, 2002; *Barreiro et al.*, 2005; *Sloan et al.*, 1996; *Haywood et al.*, 2002; *Haywood and Valdes*, 2004; *Jiang et al.*, 2005].

[3] A major conclusion of the PRISM reconstruction is that the mid-Pliocene temperature anomaly increased with latitude; that is, the poles were warmer while the tropics remained at temperatures similar to modern [*Dowsett et al.*, 1999, 2005]. In the North Atlantic, an enhanced North Atlantic Drift system may have supplied additional heat to the Norwegian and Greenland seas, contributing to the decreased mid-Pliocene equator-pole temperature gradient [*Dowsett et al.*, 1996]. However, rare SST estimates contradicting this trend appear in the PRISM data set. One such example in the North Atlantic is at Deep Sea Drilling Project (DSDP) Site 609 where the estimated SST exceeds estimates from nearby sites by ~4.5°C. The PRISM SST estimate at 609B, based on quantitative analytical techniques applied to fossil assemblages of planktic foraminifer, is seemingly anomalous. Though quantitative analytical procedures utilizing planktic foraminiferal assemblages are the convention for SST reconstructions, additional paleothermometry techniques (i.e., Mg/Ca ratios and alkenone unsaturation indices) offer alternate pathways to SST estimation.

[4] To determine if faunal-based temperature estimates are reliably estimating past SST or if they reflect a peculiarity in the SST estimation method, we compared three independently derived mid-Pliocene estimates of SST and near-surface temperature at four North Atlantic DSDP sites that transect the modern North Atlantic Drift: DSDP Hole 552A (2301 m water depth), located near the margin of the Hatton-Rockall Basin just west of Edoras Bank, and DSDP Holes 609B (3883 m water depth), 607 (3427 m water depth), and 606 (3007 m water depth), located on the flanks of the Mid-Atlantic Ridge (Figure 1).

2. Methods and Procedures

[5] Cores from DSDP Holes 552A, 609B, 607, and 606, originally sampled for faunal assemblage analysis, were resampled for alkenone and/or Mg/Ca analyses at the same sampling intervals to coincide with existing faunal samples. In two cases, data from all three proxies do not match sample intervals exactly: Alkenone data from DSDP Hole 607 were provided by K. T. Lawrence (unpublished data,

[1]U.S. Geological Survey, Reston, Virginia, USA.
[2]Division of Earth and Ocean Sciences, Nicholas School of the Environment and Earth Sciences, Duke University, Durham, North Carolina, USA.
[3]Geology and Environmental Geosciences, Lafayette College, Easton, Pennsylvania, USA.

0883-8305/08/2008PA001608$12.00

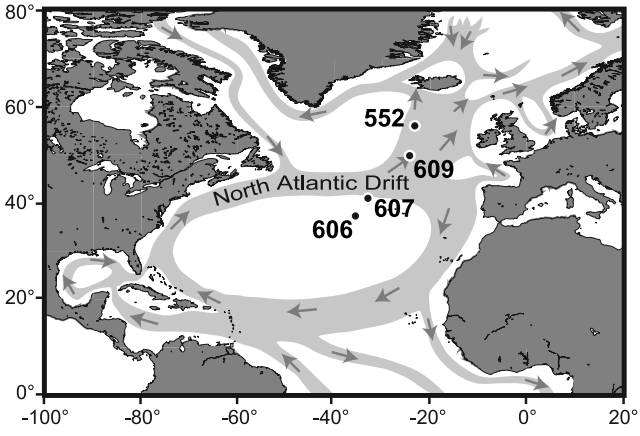

Figure 1. Location of DSDP sites utilized in this study and modern surface circulation.

2006), and Mg/Ca data from DSDP Hole 609B were obtained from *Bartoli et al.* [2005]. These data were matched to PRISM age models.

2.1. Mid-Pliocene Time Slab

[6] We follow PRISM time slab chronology, focusing on the short interval between 3.29 and 2.97 Ma for which there exists a large amount of faunal-based SST estimates. The PRISM time slab was originally established as 3.15–2.85 Ma [*Dowsett et al.*, 1994], following the timescale of *Berggren et al.* [1985]. Following the addition of the geomagnetic polarity timescale of *Berggren et al.* [1995], the astronomically tuned timescale of *Lourens et al.* [1996], and abundant data indicating warmer-than-present conditions on a global scale, the PRISM interval was revised to 3.29–2.97 Ma. The PRISM interval lies between the transition of marine oxygen isotope stages M2/M1 and G19/G18 [*Shackleton et al.*, 1995] in the middle part of the Gauss normal polarity chron (C2An) and ranges from near the bottom of C2An1 (just above Kaena reversed polarity) to within C2An2r (Mammoth reversed polarity). This interval correlates in part to planktic foraminiferal zones PL3 (*Globorotalia margaritae–Sphaeroidinellopsis seminulina* interval zone), PL4 (*Sphaeroidinellopsis seminulina–Dentoglobigerina altispira* interval zone), and PL5 (*Dentoglobigerina altispira–Globorotalia miocenica* interval zone) of *Berggren et al.* [1995]. It falls within calcareous nannofossil zone NN16 of *Martini* [1971] or CN12a of *Bukry* [1973, 1975]. Low-amplitude obliquity cycles continued throughout the mid-Pliocene while precessional cycles built in amplitude during the PRISM time slab [*Dowsett and Robinson*, 2006].

2.2. Faunal Assemblage Paleothermometry

[7] Pliocene SSTs were first reconstructed for the North Atlantic from planktic foraminiferal assemblages using quantitative micropaleontological methods by *Dowsett and Poore* [1990] and *Dowsett* [1991]. Continuing this research, the U.S. Geological Survey PRISM Project quantitatively documented mid-Pliocene warming in the North Atlantic Ocean [*Dowsett et al.*, 1992, 1994].

[8] Faunal samples used in the PRISM SST reconstruction were processed following standard low-temperature (isotopic) procedures in which samples were disaggregated in dilute sodium hexametaphosphate, dried at $\leq$50°C, and sieved into 63–150 μ and >150 μ size fractions. A split of 300 to 350 planktic foraminifer specimens was obtained from the >150 μ size fraction using a Carpco sample splitter. Specimens were assigned to 21 taxonomic categories [*Dowsett*, 1991], and counts were converted to percent data.

[9] A factor analytic transfer function (GSF18 [*Dowsett and Poore*, 1990; *Dowsett*, 1991]), calibrated to the modern SST analysis of *Reynolds and Smith* [1995], was used to transform Pliocene planktic foraminifer census data into February and August SST estimates. This technique is described in detail by *Dowsett and Poore* [1990] and *Dowsett* [1991]. Microfossil census data for the mid-Pliocene DSDP holes studied here were published previously as part of the PRISM Project [*Dowsett et al.*, 1988; *Dowsett and Poore*, 1990; *Poore*, 1991; *Dowsett and West*, 1992; *PRISM Project Members*, 1996]. Mid-Pliocene February and August SST estimates for these sites, given by *Dowsett and Poore* [1991] and *Dowsett et al.* [1999], resulted from warm peak averaging [*Dowsett and Robinson*, 2006], but SST estimates presented here differ slightly in that we calculated simple averages for each site from all samples within the PRISM time slab, without regard to warm peaks, to facilitate comparison with simple sample averages resulting from other proxies of paleotemperature.

2.3. Mg/Ca Paleothermometry

[10] The ratio of magnesium to calcium in foraminiferal tests varies exponentially with temperature [e.g., *Nürnberg et al.*, 1996; *Mashiotta et al.*, 1999; *Lea et al.*, 1999] and thus allows for temperature estimation of the water mass at the time and water depth of calcification. Approximately 60 foraminifer shells of *Globigerina bulloides, Neogloboquadrina atlantica,* and *Globigerinoides ruber* were picked from the 250 to 355 μ size fraction for Mg/Ca analysis. Mg/Ca cleaning procedures were modified from the *Boyle* [1981] cleaning method. Foraminifer shells were crushed to open chambers and then subjected to multiple rinses/sonications with deionized water and methanol and reductive and oxidative cleaning with intermittent sonication, each followed by deionized water rinses, weak acid rinses/leaches, final deionized water rinses, dissolution, centrifuging, decanting, and analysis. Aqueous solutions were analyzed for Mg and Ca simultaneously on a Fisons Instruments Spectraspan 7 Direct Current Plasma atomic emission spectrometer at Duke University using matrix-matched calibration standards mixed from ultrapure plasma-grade standard solutions. Triple-acid-washed, triple-rinsed plastic labware was used throughout the cleaning procedure and analysis.

[11] Mg/Ca–derived SST estimates were calculated for multiple species. We applied the equation developed by *Mashiotta et al.* [1999], designed for high-latitude studies of *G. bulloides*, to Mg/Ca ratios of this species to calculate

Table 1. DSDP Hole Locations and SST Estimates for Each Proxy

DSDP Hole	Latitude	Longitude	Faunal Cold SST (°C)	Mg/Ca SST (°C)	Mg/Ca Species	Alkenone SST[a] (°C)	Faunal Warm SST (°C)
552A	56.04	−23.23	11.7	14.7	*G. bulloides*[b]	16.9	20.4
				11.6	*N. atlantica* [b]		
				14.3	*N. atlantica* [c]		
				16.1	*N. atlantica* [d]		
609B	49.88	−24.24	18.2	14.2	*G. bulloides*[b]	17.5	26.4
607	41.00	−32.96	14.8	18.0	*G. bulloides*[b]	20.2	21.9
				23.4	*G. ruber*[e]		
606	37.34	−35.50	18.5	25.2	*G. ruber*[e]	22.0	25.6

[a]Alkenone calibration of *Prahl et al.* [1988].
[b]*G. bulloides* calibration of *Mashiotta et al.* [1999].
[c]*N. pachyderma* calibration of *Nürnberg* [1995].
[d]Multispecies calibration of *Anand et al.* [2003].
[e]*G. ruber* calibration of *Dekens et al.* [2002].

paleotemperatures. Mg/Ca–derived temperature estimates at DSDP 609B were provided by *Bartoli et al.* [2005], who converted Mg/Ca ratios obtained from *G. bulloides* into temperatures by applying the same equation. The equation of *Dekens et al.* [2002] was used to calculate paleotemperatures from *G. ruber*.

[12] The extinct species *N. atlantica*, a highly variable form that can be morphologically similar to both *N. pachyderma* and *G. bulloides* (and is easily misidentified as *G. bulloides*), is believed to be the cold end-member of the *Neogloboquadrina* genus [*Dowsett and Poore*, 1990]. Because *N. atlantica* is extinct and no specific calibration exists, we calculated temperatures from the Mg/Ca values obtained from *N. atlantica* using the following three calibrations for comparison: (1) the equation developed by *Mashiotta et al.* [1999] designed for high-latitude studies of *G. bulloides*, (2) the *Nürnberg* [1995] equation developed for high-northern-latitude studies of *N. pachyderma,* and (3) the multispecies calibration equation developed by *Anand et al.* [2003] that is presumably more useful for extinct species.

2.4. Alkenone Unsaturation Index Paleothermometry

[13] Alkenones are produced by a few species of haptophyte algae that live in the near-surface ocean. The $U^{k'}_{37}$ index has been linearly calibrated to ocean near-surface temperature [*Prahl et al.*, 1988; *Müller et al.*, 1998; *Conte et al.*, 2006] and is used here to estimate mean annual SST. All reported $U^{k'}_{37}$ SST estimates in this study were obtained using the *Prahl et al.* [1988] calibration curve. Global core top calibration studies [*Müller et al.*, 1998; *Conte et al.*, 2006], which include sites spanning the entire range of temperatures and geographic distribution of alkenone-producing species, yield calibrations that are essentially the same as that of *Prahl et al.* [1988], indicating the global applicability of this calibration curve. These global calibration data sets include samples taken from regions of the ocean dominated by *Gephyrocapsa oceanica* [*Müller et al.*, 1998; *Conte et al.*, 2006], the most likely dominant alkenone-producing species before the Pleistocene evolution of *Emiliani huxleyi* [*Thierstein et al.*, 1977; *Bollmann et al.*, 1998]. Because the $U^{k'}_{37}$ index for sites that today are dominated by Gephyrocapsid production fall on the modern global calibration curve [*Müller et al.*, 1998; *Conte et al.*, 2006], we assume that this modern calibration applies to all values of the $U^{k'}_{37}$ index determined here.

[14] Sediment samples (~5 g) were freeze-dried and homogenized in preparation for the analysis of alkenones. Lipid extracts were extracted in 100% dichloromethane using a Dionex automated solvent extractor (ASE 200). The ASE 200 exposes each sample to a small volume of solvent (~25 mL) at elevated pressure (1.034212×10^7 Pa) and temperature (150°C). After evaporation under an N_2 stream and dilution with a small volume of toluene (~0.2 mL), the extracts were analyzed using a Hewlett-Packard 6890 gas chromatograph equipped with a flame ionization detector and a DB-1 column (60 m × 0.32 m × 0.10 μm file thickness) (J and W Scientific). The temperature program used to quantify alkenones starts at 90°C holding for 2 min, then ramps to 250°C at 40°C/min, followed by a slow ramp of 1°C/min to 300°C, and finishes with an isothermal holding step at 320°C for 11 min. Peak areas of $C_{37:2}$ and $C_{37:3}$ alkenones were determined using Hewlett-Packard Chemstation software and were used to calculate the alkenone unsaturation ($U^{k'}_{37}$) index. Reproducibility of analysis was better than ±0.005 $U^{k'}_{37}$ units, which corresponds to a temperature uncertainty of ±0.2°C using the calibration of *Prahl et al.* [1988].

2.5. Multiproxy Temperature Estimate Anomalies

[15] Direct comparison of temperature estimates from multiple proxies may be inappropriate because of the different environmental parameters measured by each proxy (i.e., depth and seasonality), even in cases where temperature estimations from all proxies were performed on the same sample, and because of the different modern SST data sets used in proxy calibrations. Therefore, in addition to reporting temperature estimates from individual proxies, we also report temperature anomalies (mid-Pliocene minus modern) to remove differences inherent in proxy calibrations and to correct for seasonality and water column depth where appropriate. In calculating alkenone-derived and Mg/Ca–derived temperature anomalies, we used modern SST values from *Levitus and Boyer* [1994], and for faunal-based anomalies, we used modern February and August SST values from *Reynolds and Smith* [1995] because these

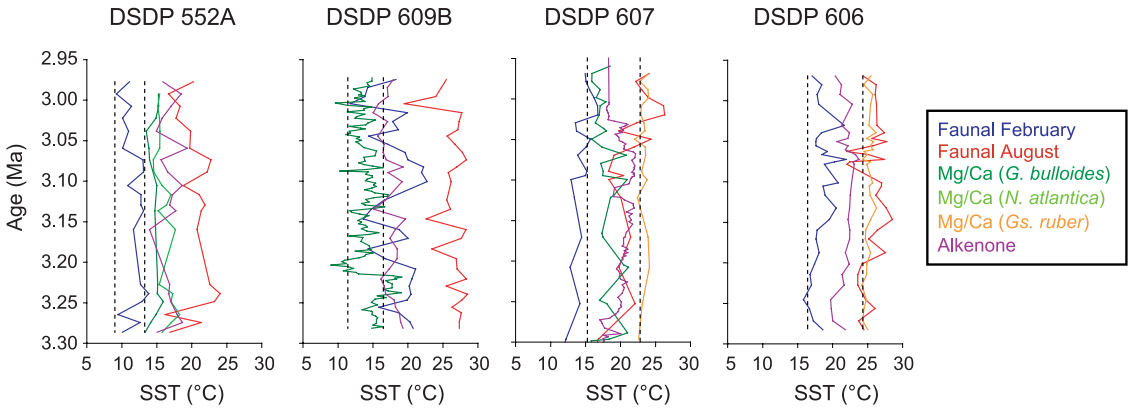

Figure 2. Mid-Pliocene SST estimates from multiple proxies for DSDP Holes 552A, 609B, 607, and 606 plotted against age (timescale of *Berggren et al.* [1995]). Vertical dashed lines are modern February and August SSTs from *Reynolds and Smith* [1995].

respective modern temperature data sets were used for the individual proxy calibrations.

3. Results

[16] Mid-Pliocene SST and near-surface temperature estimates for DSDP Holes 552A, 609B, 607, and 606, derived from multiple proxies, are listed in Table 1 as averages over the time interval and are shown graphically in Figure 2. Temperature anomalies (mid-Pliocene temperature estimate minus modern temperature) are listed in Table 2 as averages over the time interval and are shown graphically in Figure 3.

[17] At DSDP Hole 552A, the Mg/Ca–derived temperature estimate from *G. bulloides* (14.7°C) and the alkenone-derived temperature estimate (16.9°C) fall between faunal-based cold (11.7°C) and warm season (20.4°C) SST estimates. Temperature estimates based on *N. atlantica* Mg/Ca are 11.6°C, 14.3°C, and 16.1°C; differences are due to the calibration equation used for this extinct species. Only the lowest temperature estimate, calculated by applying the *G. bulloides* equation, is outside the faunal-based temperature range. These independent proxies indicate a mid-Pliocene SST anomaly of +2.6°C in February and +7.1°C in August, with a mean annual anomaly of +5.3°C. An additional mean annual anomaly of +4.9°C at 30 m water depth is recorded here. A warming of between 0.0°C and 5.6°C is also indicated at 0 to 50 m water depth from the extinct species *N. atlantica*.

[18] At DSDP Hole 609B, the Mg/Ca–derived temperature estimate for *G. bulloides* (14.2°C) and the alkenone-derived temperature estimate (17.5°C) indicate less mid-Pliocene warming than faunal-based cold (18.2°C) and warm season (26.4°C) SST estimates, thus falling outside the PRISM SST range at this site. While faunal-based SST anomalies are +6.7°C in February and +9.8°C in August, the additional independent proxies indicate a mean annual SST anomaly of only +3.4°C and warming at 30 m depth of 2.1°C.

[19] At DSDP Hole 607, the Mg/Ca–derived temperature estimate from *G. bulloides* (18.0°C) and the alkenone-derived temperature estimate (20.2°C) fall between the faunal-based cold (14.8°C) and warm season (21.9°C) SST estimates. The Mg/Ca–derived temperature estimate from *G. ruber* (23.4°C) exceeds estimates from other proxies. These independent proxies indicate a mid-Pliocene SST anomaly ranging from −1.0°C to +4.6°C and a temperature anomaly at 30 m depth of −0.8°C.

[20] At DSDP Hole 606, the Mg/Ca–derived temperature estimate from *G. ruber* (25.2°C) and the alkenone-derived temperature estimate (22.0°C) are bracketed by the faunal-based cold (18.5°C) and warm season (25.6°C) SST estimates. These independent proxies indicate a mid-Pliocene SST anomaly of between +1.1°C and +4.7°C.

[21] In general, these results show keen agreement among paleotemperature proxies at DSDP Holes 552A, 607, and

Table 2. Mid-Pliocene SST Anomalies[a]

DSDP Hole	Faunal Cold ΔSST (°C)	Mg/Ca ΔSST (°C)	Mg/Ca ΔSST[b] (°C)	Mg/Ca Species	Alkenone ΔSST (°C)	Faunal Warm ΔSST (°C)
552A	2.6	3.1	4.9	*G. bulloides*	5.3	7.1
		0.0	1.1	*N. atlantica*		
		2.7	3.8	*N. atlantica*		
		4.5	5.6	*N. atlantica*		
609B	6.7	0.1	2.1	*G. bulloides*	3.4	9.8
607	−0.5	−0.8	1.9	*G. bulloides*	1.4	−1.0
		4.6	4.6	*G. ruber*		
606	2.0	4.7	4.7	*G. ruber*	1.5	1.1

[a]Mid-Pliocene minus modern SST.
[b]Corrected for species calcification depth: 30 m for *G. bulloides*, 50 m for *N. atlantica*, and 0 m for *G. ruber*.

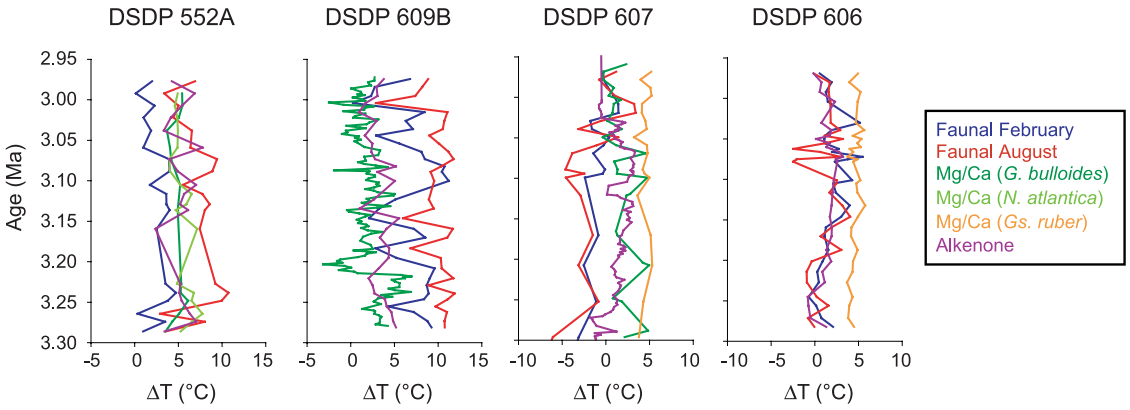

Figure 3. Mid-Pliocene SST anomalies from multiple proxies for DSDP Holes 552A, 609B, 607, and 606 plotted against age (timescale of *Berggren et al.* [1995]).

606, with the understanding that temperature estimates from individual proxies reflect different seasons of production and positions in the water column of the producing organisms. Alkenone-based and Mg/Ca–derived temperature estimates at DSDP Hole 609B, however, diverge from faunal-based temperature estimates at that site.

4. Discussion

[22] The multiproxy approach to paleotemperature estimation is complicated in that each proxy records a different aspect of mixed layer conditions, making direct comparisons of SST estimates impractical. Existing faunal-based SST estimates, calculated by applying a transfer function to species assemblage data, provide cold and warm season temperatures that define a range of annual surface conditions. Mg/Ca–derived temperature estimates reflect conditions at the preferred calcification depth and season of the individual foraminifer species studied. Alkenone-derived SST estimates are linked to the timing of plankton blooms which varies with latitude. In the North Atlantic Drift province, phytoplankton maxima occur in the spring and fall [*Dandonneau et al.*, 2004], and, therefore, alkenone-derived SST estimates most likely record mean annual conditions. Though complicated, evaluation of temperature estimates from distinct proxies at a single location increases confidence in results by reducing errors [*Mix et al.*, 2000] and permits seasonality studies and surface water structure reconstructions [*Bard*, 2001]. Also, when temperature estimates clearly disagree with one another, the multiproxy approach helps describe the limitations of each proxy method [*Mix et al.*, 2000].

4.1. Exaggerated Faunal-Based SST Estimates

[23] At DSDP Hole 609B, faunal-based SST estimates indicate a pronounced mid-Pliocene warming exceeding the warming recorded by other proxies at this site and by all proxies at other North Atlantic sites (Figure 4). Faunal assemblages at Hole 609B are characterized by high abundances of *Globorotalia puncticulata* (up to 62%, 28% averaged over the interval) and *Neogloboquadrina acostaensis* (up to 50%, 25% averaged over the interval). It is unlikely that the high abundances of these two species are due to dissolution. Planktic to benthic foraminiferal ratios far below 100 are considered an indicator of dissolution [*Berger*, 1967, 1970], but the average ratio at Hole 609B over this interval is 117. Also, *Raymo et al.* [1987] docu-

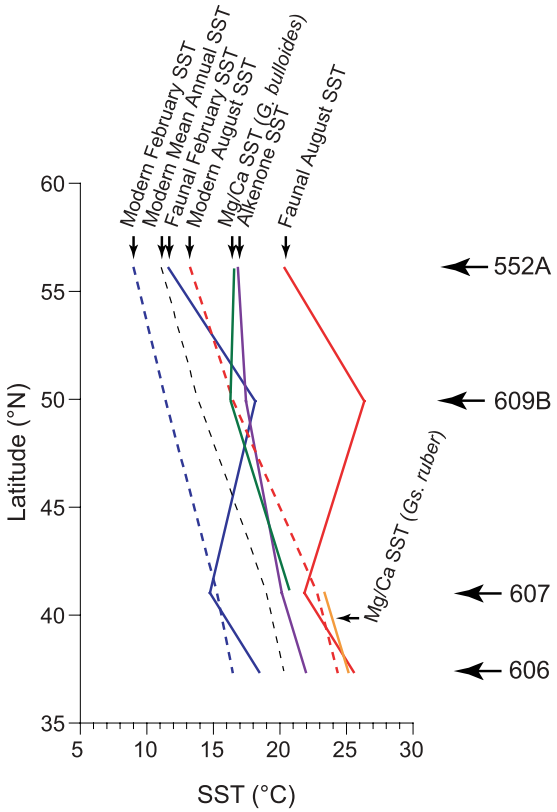

Figure 4. Comparison of mid-Pliocene SST estimates from multiple proxies and modern February and August SSTs along the four DSDP sites in the North Atlantic transect. Faunal-based SST estimates are warmer at DSDP 609B and cooler at DSDP 607 than expected of a smooth temperature gradient.

mented many high-amplitude changes in relative abundances of these and other species at Hole 609B prior to 2.45 Ma and attributed them to movement of the North Atlantic Drift not to dissolution.

[24] SST estimates derived from both *G. puncticulata* and *N. acostaensis*, which are now extinct, are based upon ecological analogy to extant taxa *Globorotalia inflata* and *Neogloboquadrina dutertrei*, respectively, that show modern distributions southward of their mid-Pliocene counterparts [*Dowsett and Robinson*, 2007]. While other faunal and floral proxies in the northeast Atlantic corroborate significant warming [e.g., *Cronin*, 1991a, 1991b; *Willard*, 1994; *Dowsett et al.*, 1994; *Dowsett*, 2007], it is possible that the high abundances of *N. acostaensis* and *G. puncticulata* drive the faunal transfer function to overestimate warming in the region.

[25] Along with other subsurface dwellers that show elevated abundance at this time, these species may also be indicating an important event in the water column not directly related to SST. For example, *N. dutertrei*, the extant ancestor of *N. acostaensis* [*Kennett and Srinivasan*, 1983; *Bolli and Saunders*, 1985], is a modern indicator of ocean productivity [*Duplessy et al.*, 1981]. At Site 609, *N. dutertrei* represents only 3.3% of the modern core top assemblage, but *N. acostaensis* composes 25% of the mid-Pliocene assemblage, perhaps indicating much stronger productivity at this site during the mid-Pliocene. Misinterpretation of this productivity signal may have augmented the warming indicated by the transfer function.

4.2. Seasonality and Depth Effects of Mg/Ca–Derived Temperature Estimates

[26] Depth stratification of planktic foraminifer species is closely related to thermohaline stratification [*Savin et al.*, 1985; *Chaisson*, 1995]. Generally, spinose, globigerine forms populate the surface water, while nonspinose, globorotaliid forms are thermocline or deeper dwelling [*Douglas and Savin*, 1978; *Leckie*, 1989; *Gasperi and Kennett*, 1993]. In the modern ocean, calcification seasons and depths vary with location and with species. Mg/Ca in *G. bulloides* represents average spring to summer temperature values of the upper 60 m of the water column in the midlatitude North Atlantic [*Ottens*, 1992; *Schiebel et al.*, 1997]. *Elderfield and Ganssen* [2000] found seasonal effects in the Mg/Ca of *G. bulloides* in a core top study of calcification temperatures in the North Atlantic: between 30° and 40°N, *G. bulloides* records February to March SST, while above 40°N, *G. bulloides* records April to June SST. *G. ruber* calcifies between 0 and 50 m water depth [*Anand et al.*, 2003], but Mg/Ca of *G. ruber* records mean annual SST in the tropical and subtropical Atlantic [*Dekens et al.*, 2002].

[27] Accordingly, Mg/Ca of *G. bulloides* should record April to June SST, and Mg/Ca of *G. ruber* should record mean annual SST at Site 607, but Mg/Ca–derived SST estimates based on *G. ruber* are 5.4°C higher than those based on *G. bulloides* (Table 1). To explain this difference, we suggest that Mg/Ca–derived SST estimates based on *G. ruber* more closely reflect faunal-based SST estimates for August, while those based on *G. bulloides* may reflect either early spring SST or mean annual temperatures at some depth (Figure 4). Table 2 lists temperature anomalies for *G. bulloides* Mg/Ca calculated as mid-Pliocene SST estimate minus modern SST and as mid-Pliocene SST estimate minus modern temperature at 30 m water depth.

4.3. Extinct Species in Mg/Ca–Derived SST Estimates

[28] Using extinct species to estimate SST is of concern because of necessary assumptions regarding habitat preferences. We use *N. atlantica*, a dominant species in the high latitudes during the Pliocene but absent or very rare in midlatitudes to low latitudes [*Poore and Berggren*, 1975; *Poore*, 1981; *Raymo et al.*, 1987], for Mg/Ca analysis because of its abundance in North Atlantic sediments. *Dowsett and Poore* [1990] grouped *N. atlantica* with *N. pachyderma* in a "cool" *Neogloboquadrina* category for the purposes of faunal-based SST estimation.

[29] In estimating paleotemperatures from Mg/Ca, *N. atlantica* yields temperatures 3.1°C cooler than *G. bulloides* when the same calibration equation [*Mashiotta et al.*, 1999] is used for both species (Table 1), supporting the placement of *N. atlantica* as the cold end-member of the *Neogloboquadrina* genus and identifying it as a species ecologically distinct from *G. bulloides*. Clearly, the *G. bulloides* equation is not appropriate for paleotemperature estimation using *N. atlantica*.

[30] *N. atlantica* Mg/Ca temperature estimates resulting from the *N. pachyderma* equation of *Nürnberg* [1995] are 0.4°C cooler than estimates from *G. bulloides* from the same samples. *N. pachyderma,* an extant relative of *N. atlantica*, occurs mainly between 50 and 100 m water depth in high latitudes, but Mg/Ca in *N. pachyderma,* when converted to temperature using the *Nürnberg* [1995] equation, should reflect SST [*Nürnberg*, 1995]. As is the case for *G. bulloides,* our Mg/Ca–derived SST estimates based on *N. atlantica*, calculated using the *Nürnberg* [1995] equation, may reflect either early spring SST or mean annual temperatures at some depth, thus explaining the cooler temperature estimates. Table 2 lists temperature anomalies for *N. atlantica* Mg/Ca at the surface and corrected for 50 m water depth. However, the multispecies calibration equation of *Anand et al.* [2003] yields *N. atlantica* Mg/Ca–derived temperature estimates that are 1.4°C warmer than estimates from *G. bulloides* from the same samples and may reflect mean annual SST based on the agreement with other proxies at Hole 552A (Table 1 and Figure 2).

4.4. Revised North Atlantic Mid-Pliocene SST Estimates

[31] SST estimates from the three independent proxies at each of the four North Atlantic sites are compared to modern SST in Figure 4. Mg/Ca–derived and alkenone-derived estimates increasingly warm with latitude as compared to modern. Faunal-based SST estimates follow the same pattern if estimates at Site 609 are ignored. Though the proxies differ in estimating SST values, they agree in that each produces a reduced mid-Pliocene SST gradient.

[32] The averaged multiproxy SST estimates improve PRISM faunal-based estimates that may have been exaggerated by high abundances of extinct species and/or a high-

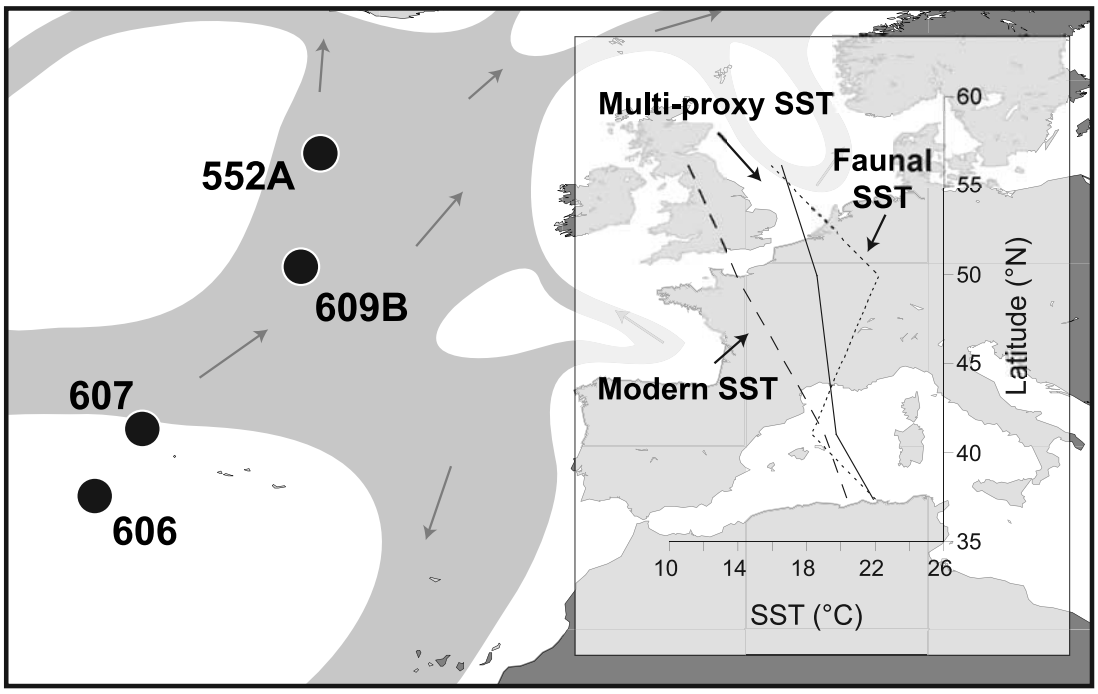

Figure 5. Revised SST estimates based on multiple proxies for DSDP Holes 552A, 609B, 607, and 606 compared to faunal-based SST estimates and modern SSTs along the North Atlantic transect.

productivity signal; they also support the PRISM faunal-based estimates and corroborate mid-Pliocene warming that increases with latitude (Figure 5). *Dowsett et al.* [1992] suggested, on the basis of the reduced mid-Pliocene pole to equator surface temperature gradient, relative to today, that meridional ocean heat transport was the cause of mid-Pliocene warming, and this conclusion is supported by the multiproxy data presented here.

4.5. SST Estimation in the High Latitudes

[33] Because of the high sensitivity displayed by polar regions during the current warming trend, accurate reconstructions of paleoconditions in high-latitude regions are integral to reliable mid-Pliocene reconstructions. Additional SST estimates from the high latitudes are necessary to better understand the degree, extent, and cause of mid-Pliocene warming, but traditional faunal-based techniques are not well suited for estimating SST in high latitudes where foraminifer specimens are often scarce and where assemblages become monospecific. Mg/Ca and alkenone paleothermometry are better suited than faunal-based methods for characterizing past ocean surface temperatures in cold, high-latitude regions where foraminifera are rare.

[34] Extending the relationship among proxies northward of DSDP Site 552 is possible through understanding the effectiveness and limitations of individual proxy methods under various oceanographic conditions and the relationship among proxies at sites where all three proxies exist. The relationship between *N. atlantica* Mg/Ca and mean annual SST presented here may help extend this proxy method into previously unobtainable high-latitude regions where mid-Pliocene faunal assemblages are dominated by this extinct species. By extending northward the annual range of SSTs provided by the faunal-based transfer function at DSDP Site 552, mean annual SST estimates based on alkenones and Mg/Ca can be converted into estimates for February and August at high-latitude sites.

5. Conclusions

[35] Combining faunal-based SST estimates with independent geochemical (Mg/Ca and alkenone unsaturation indices) proxies of SST reduces the error associated with the previous SST reconstruction of the North Atlantic based only on foraminiferal assemblages. Faunal analyses had shown a reduced mid-Pliocene gradient in the North Atlantic as higher-latitude sites experienced more warming relative to modern than lower-latitude sites [*Dowsett et al.*, 1992]. This multiproxy study corroborates and better constrains mid-Pliocene warming that increases with latitude and supports the claim that meridional heat transport was at least in part responsible for mid-Pliocene warmth.

[36] Because each proxy records a different aspect of surface ocean conditions, evaluation of temperature estimates from multiple proxies promises to improve SST reconstructions by refining surface condition estimates by addressing seasonality and depth parameters of the different proxy organisms. In addition, understanding the seasonal, depth, and temperature relationships among proxies at sites where all three proxies exist not only allows us to reconcile disagreements among proxies when necessary but also to extend this understanding to higher latitudes and other

regions where traditional faunal-based SST estimates are not well suited because of reduced foraminifer populations.

[37] Differences among SST estimates from multiple proxies are expected because each proxy defines the temperature of the water column at a specific depth and/or season. A seasonal comparison of time-averaged temperature anomalies at the appropriate depth for each proxy is more suitable and more useful in estimating SSTs of the mid-Pliocene.

[38] Under certain conditions, paleotemperature proxies respond to factors other than temperature. The use of multiple proxies illuminates proxy responses to high abundances of extinct species and/or to changes in nutrients that may have been misinterpreted as temperature signals.

[39] Additional SST estimates in the high latitudes are necessary for a more complete and reliable mid-Pliocene SST reconstruction. The relationship among proxies presented here will aid in extending SST estimates, mean annual and seasonal, into high-latitude regions where foraminifera are absent, rare, or dominantly *N. atlantica*.

[40] **Acknowledgments.** This paper benefited from discussions with Tom Cronin and Matt Wright. We thank Rocío Caballero for help with various aspects of technical assistance. This work is a product of the U.S. Geological Survey Earth Surface Dynamics Program. We thank the Ocean Drilling Program for the provision of samples. ODP is sponsored by the U.S. National Science Foundation and participating countries under the management of Joint Oceanographic Institutions. We thank E. Kandiano and an anonymous reviewer for comments and suggestions that improved the quality of this paper. G.S.D. was supported by NSF grant ATM-0323276.

References

Anand, P., H. Elderfield, and M. H. Conte (2003), Calibration of Mg/Ca thermometry in planktonic foraminifera from a sediment trap time series, *Paleoceanography*, *18*(2), 1050, doi:10.1029/2002PA000846.

Bard, E. (2001), Comparison of alkenone estimates with other paleotemperature proxies, *Geochem. Geophys. Geosyst.*, *2*(1), 1002, doi:10.1029/2000GC000050.

Barreiro, M., G. Philander, R. Pacanowski, and A. Fedorov (2005), Simulations of warm tropical conditions with application to middle Pliocene atmospheres, *Clim. Dyn.*, *26*, 349–365, doi:10.1007/s00382-005-0086-4.

Bartoli, G., M. Sarnthein, M. Weinelt, H. Erlenkeuser, D. Garbe-Schönberg, and D. W. Lea (2005), Final closure of Panama and the onset of Northern Hemisphere glaciation, *Earth Planet. Sci. Lett.*, *237*, 33–44, doi:10.1016/j.epsl.2005.06.020.

Berger, W. H. (1967), Foraminiferal ooze: Solution at depths, *Science*, *156*, 383–385, doi:10.1126/science.156.3773.383.

Berger, W. H. (1970), Planktonic foraminifera: Selective solution and the lysocline, *Mar. Geol.*, *8*, 111–138, doi:10.1016/0025-3227(70)90001-0.

Berggren, W. A., D. V. Kent, and J. van Couvering (1985), The Neogene: Part 2. Neogene geochronology and chronostratigraphy, in *The Chronology of the Geological Record*, *Geol. Soc. Mem.*, vol. 10, edited by N. J. Snelling, pp. 211–260, Blackwell Sci., Malden, Mass.

Berggren, W. A., D. V. Kent, C. C. Swisher, and M.-P. Aubry (1995), A revised Cenozoic geochronology and chronostratigraphy, in *Geochronology, Time Scales and Global Stratigraphic Correlation*, edited by W. A. Berggren et al., *Spec. Publ. SEPM Soc. Sediment. Geol.*, *54*, 129–212.

Bolli, H. M., and J. B. Saunders (1985), Oligocene to Holocene low latitude planktic foraminifera, in *Plankton Stratigraphy*, *Cambridge Earth Sci. Ser.*, vol. 1, edited by H. M. Bolli, J. B. Saunders, and K. Perch-Nielsen, pp. 155–262, Cambridge Univ. Press, New York.

Bollmann, J., K.-H. Baumann, and H. R. Thierstein (1998), Global dominance of *Gephyrocapsa* coccoliths in the late Pleistocene: Selective dissolution, evolution, or global environmental change?, *Paleoceanography*, *13*, 517–529, doi:10.1029/98PA00610.

Boyle, E. A. (1981), Cadmium, zinc, copper and barium in foraminifera tests, *Earth Planet. Sci. Lett.*, *53*, 11–35, doi:10.1016/0012-821X(81)90022-4.

Bukry, D. (1973), Low-latitude coccolith biostratigraphic zonation, *Initial Rep. Deep Sea Drill. Proj.*, *15*, 685–703.

Bukry, D. (1975), Coccolith and silicoflagellate stratigraphy, northwestern Pacific Ocean, Deep Sea Drilling Project Leg 32, *Initial Rep. Deep Sea Drill. Proj.*, *32*, 677–701.

Chaisson, W. (1995), Planktonic foraminiferal assemblages and paleoceanographic change in the trans-tropical Pacific Ocean: A comparison of west (Leg 130) and east (Leg 138), latest Miocene to Pleistocene, *Proc. Ocean Drill. Program Sci. Results*, *138*, 555–597.

Chandler, M., D. Rind, and R. Thompson (1994), Joint investigations of the middle Pliocene climate: II. GISS GCM Northern Hemisphere results, *Global Planet. Change*, *9*, 197–219, doi:10.1016/0921-8181(94)90016-7.

Conte, M. H., M.-A. Sicre, C. Rühlemann, J. C. Weber, S. Schulte, D. Schulz-Bull, and T. Blanz (2006), Global temperature calibration of the alkenone unsaturation index (Uk'_{37}) in surface waters and comparison with surface sediments, *Geochem. Geophys. Geosyst.*, *7*, Q02005, doi:10.1029/2005GC001054.

Cronin, T. M. (1991a), Late Neogene marine ostracoda from Tjörnes, Iceland, *J. Paleontol.*, *65*, 767–794.

Cronin, T. M. (1991b), Pliocene shallow water paleoceanography of the North Atlantic Ocean based on marine ostracodes, *Quat. Sci. Rev.*, *10*, 175–188, doi:10.1016/0277-3791(91)90017-O.

Dandonneau, Y., P. Deschamps, J. Nicolas, H. Loisel, J. Blanchot, Y. Montel, F. Thieuleux, and G. Bécu (2004), Seasonal and interannual variability of ocean color and composition of phytoplankton communities in the North Atlantic, equatorial Pacific and South Pacific, *Deep Sea Res., Part II*, *51*, 303–318, doi:10.1016/j.dsr2.2003.07.018.

Dekens, P. S., D. W. Lea, D. K. Pak, and H. J. Spero (2002), Core top calibration of Mg/Ca in tropical foraminifera: Refining paleotemperature estimation, *Geochem. Geophys. Geosyst.*, *3*(4), 1022, doi:10.1029/2001GC000200.

Douglas, R. G., and S. M. Savin (1978), Oxygen isotopic evidence for the depth stratification of Tertiary and Cretaceous planktic foraminifera, *Mar. Micropaleontol.*, *3*, 175–196, doi:10.1016/0377-8398(78)90004-X.

Dowsett, H. J. (1991), The development of a long-range foraminifer transfer function and application to late Pleistocene North Atlantic climatic extremes, *Paleoceanography*, *6*, 259–273, doi:10.1029/90PA02541.

Dowsett, H. J. (2007), The PRISM palaeoclimate reconstruction and Pliocene sea-surface temperature, in *Deep-Time Perspectives on Climate Change: Marrying the Signal From Computer Models and Biological Proxies*, *Micropalaeontol. Soc. Spec. Publ.*, vol. TMS002, edited by M. Williams et al., pp. 459–480, The Geol. Soc., London.

Dowsett, H. J., and R. Z. Poore (1990), A new planktic foraminifer transfer function for estimating Pliocene-Holocene sea surface temperatures, *Mar. Micropaleontol.*, *16*, 1–23, doi:10.1016/0377-8398(90)90026-I.

Dowsett, H. J., and R. Z. Poore (1991), Pliocene sea surface temperatures of the North Atlantic Ocean at 3.0 Ma, *Quat. Sci. Rev.*, *10*, 189–204, doi:10.1016/0277-3791(91)90018-P.

Dowsett, H. J., and M. M. Robinson (2006), Stratigraphic framework for Pliocene paleoclimate reconstruction: The correlation conundrum, *Stratigraphy*, *3*, 53–64.

Dowsett, H. J., and M. M. Robinson (2007), Mid-Pliocene planktic foraminifer assemblage of the North Atlantic Ocean, *Micropaleontology*, *53*, 105–126.

Dowsett, H. J., and S. M. West (1992), Pliocene planktic foraminifer census data from Deep Sea Drilling Project Hole 607 and Ocean Drilling Program Hole 661A, *U.S. Geol. Surv. Open File Rep., 92–413*, 4 pp.

Dowsett, H. J., L. B. Gosnell, and R. Z. Poore (1988), Pliocene planktic foraminifer census data from Deep Sea Drilling Project Holes 366A, 410, 606, and 646B, *U.S. Geol. Surv. Open File Rep., 88–654*, 14 pp.

Dowsett, H. J., T. M. Cronin, R. Z. Poore, R. S. Thompson, R. C. Whatley, and A. M. Wood (1992), Micropaleontological evidence for increased meridional heat transport in the North Atlantic Ocean during the Pliocene, *Science*, *258*, 1133–1135, doi:10.1126/science.258.5085.1133.

Dowsett, H. J., R. S. Thompson, J. A. Barron, T. M. Cronin, R. F. Fleming, S. E. Ishman, R. Z. Poore, D. A. Willard, and T.R. Holtz Jr. (1994), Paleoclimatic reconstruction of a warmer Earth: PRISM middle Pliocene Northern Hemisphere synthesis, *Global Pla-*

net. Change, *9*, 169–195, doi:10.1016/0921-8181(94)90015-9.

Dowsett, H., J. Barron, and R. Poore (1996), Middle Pliocene sea surface temperatures: A global reconstruction, *Mar. Micropaleontol.*, *27*, 13–25, doi:10.1016/0377-8398(95)00050-X.

Dowsett, H. J., J. A. Barron, R. Z. Poore, R. S. Thompson, T. M. Cronin, S. E. Ishman, and D. A. Willard (1999), Middle Pliocene Paleoenvironmental Reconstruction: PRISM2, *U.S. Geol. Surv. Open File Rep., 99–535*. (Available at http://pubs.usgs.gov/openfile/of99-535)

Dowsett, H. J., M. A. Chandler, T. M. Cronin, and G. S. Dwyer (2005), Middle Pliocene sea surface temperature variability, *Paleoceanography*, *20*, PA2014, doi:10.1029/2005PA001133.

Duplessy, J. C., A. W. H. Bé, and P. L. Blanc (1981), Oxygen and carbon isotopic composition and biogeographic distribution of planktonic foraminifera in the Indian Ocean, *Palaeogeogr. Palaeoclimatol. Palaeoecol.*, *33*, 9–46, doi:10.1016/0031-0182(81)90031-6.

Elderfield, H., and G. Ganssen (2000), Past temperature and $\delta^{18}O$ of surface ocean waters inferred from foraminiferal Mg/Ca ratios, *Nature*, *405*, 442–445, doi:10.1038/35013033.

Gasperi, J. T., and J. P. Kennett (1993), Miocene planktonic foraminifers at DSDP Site 289: Depth stratification using isotopic differences, *Proc. Ocean Drill. Program Sci. Results*, *130*, 323–332.

Haywood, A. M., and P. J. Valdes (2004), Modeling Pliocene warmth: Contributions of atmosphere, oceans, and cryosphere, *Earth Planet. Sci. Lett.*, *218*, 363–377, doi:10.1016/S0012-821X(03)00685-X.

Haywood, A. M., P. J. Valdes, J. E. Francis, and B. W. Sellwood (2002), Global middle Pliocene biome reconstruction: A data/model synthesis, *Geochem. Geophys. Geosyst.*, *3*(12), 1072, doi:10.1029/2002GC000358.

Intergovernmental Panel on Climate Change (2001), *Climate Change 2001: The Science of Climate Change: Contribution of Working Group I to the Third Assessment Report of the Intergovernmental Panel on Climate Change*, edited by J. T. Houghton et al., 881 pp., Cambridge Univ. Press, Cambridge, U. K.

Jiang, D., H. Wang, Z. Ding, X. Lang, and H. Drange (2005), Modeling the middle Pliocene climate with a global atmospheric general circulation model, *J. Geophys. Res.*, *110*, D14107, doi:10.1029/2004JD005639.

Kennett, J. P., and M. S. Srinivasan (1983), *Neogene Planktonic Foraminifera: A Phylogenetic Atlas*, 230 pp., Hutchinson Ross, Stroudsburg, Pa.

Lea, D. W., T. A. Mashiotta, and H. J. Spero (1999), Controls on magnesium and strontium uptake in planktonic foraminifera determined by live culturing, *Geochim. Cosmochim. Acta*, *63*, 2369–2379, doi:10.1016/S0016-7037(99)00197-0.

Leckie, R. M. (1989), An oceanographic model for the early evolutionary history of planktonic foraminifera, *Palaeogeogr. Palaeoclimatol. Palaeoecol.*, *73*, 107–138, doi:10.1016/0031-0182(89)90048-5.

Levitus, S., and T. P. Boyer (1994), *World Ocean Atlas 1994,* vol. 4, *Temperature*, *NOAA Atlas NESDIS*, vol. 4, 129 pp., NOAA, Silver Spring, Md.

Lourens, L. J., A. Antonarakou, F. J. Hilgen, and W. J. Zachariasse (1996), Evaluation of the Plio-Pleistocene astronomical timescale, *Paleoceanography*, *11*, 391–413, doi:10.1029/96PA01125.

Martini, E. (1971), Standard Tertiary and Quaternary calcareous nannoplankton zonation, in *Proceedings of the Second Planktonic Conference, Roma, 1970*, vol. 2, edited by A. Farinacci, pp. 739–785, Technoscienza, Rome.

Mashiotta, A. T., D. W. Lea, and H. J. Spero (1999), Glacial-interglacial changes in subantarctic sea surface temperature and $\delta^{18}O$ -water using foraminiferal Mg, *Earth Planet. Sci. Lett.*, *170*, 417–432, doi:10.1016/S0012-821X(99)00116-8.

Mix, A. C., E. Bard, G. Elginton, L. D. Keigwin, A. C. Ravelo, and Y. Rosenthal (2000), Alkenones and multiproxy strategies in paleoceanographic studies, *Geochem. Geophys. Geosyst.*, *1*(11), 1033, doi:10.1029/2000GC000056.

Molnar, P., and M. A. Cane (2002), El Niño's tropical climate and teleconnections as a blueprint for pre-Ice Age climates, *Paleoceanography*, *17*(2), 1021, doi:10.1029/2001PA000663.

Müller, P. J., G. Kirst, G. Ruhland, I. von Storch, and A. Rosell-Melé (1998), Calibration of the alkenone paleotemperature index $U^{K'}_{37}$ based on core-tops from the eastern South Atlantic and the global ocean (60°N–60°S), *Geochim. Cosmochim. Acta*, *62*, 1757–1772, doi:10.1016/S0016-7037(98)00097-0.

Nürnberg, D. (1995), Magnesium in tests of *Neogloboquadrina pachyderma* (sinistral) from high northern and southern latitudes, *J. Foraminiferal Res.*, *25*, 350–368.

Nürnberg, D., J. Bijma, and C. Hemleben (1996), Assessing the reliability of magnesium in foraminiferal calcite as a proxy for water mass temperatures, *Geochim. Cosmochim. Acta*, *60*, 803–814, doi:10.1016/0016-7037(95)00446-7.

Ottens, J. J. (1992), Planktic foraminifera as indicators of ocean environments in the northeast Atlantic, Ph.D. thesis, Free Univ. of Amsterdam, Enschede, Netherlands.

Poore, R. Z. (1981), Temporal and spatial distribution of ice rafted mineral grains in Pliocene sediments of the North Atlantic: Implications for Late Cenozoic climate history, *Spec. Publ. Soc. Econ. Paleontol. Mineral.*, *32*, 505–515.

Poore, R. Z. (1991), Pliocene planktic foraminifer census data from Deep Sea Drilling Project Hole 603C, *U.S. Geol. Surv. Open File Rep., 91–309*, 7 pp.

Poore, R. Z., and W. A. Berggren (1975), The morphology and classification of Neogloboquadrina atlantica (Berggren), *J. Foraminiferal Res.*, *5*, 76–84.

Prahl, F. G., L. A. Muehlhausen, and D. L. Zahnle (1988), Further evaluation of long-chain alkenones as indicators of paleoceanographic conditions, *Geochim. Cosmochim. Acta*, *52*, 2303–2310, doi:10.1016/0016-7037(88)90132-9.

PRISM Project Members (1996), Pliocene planktic foraminifer census data from the North Atlantic region, *U.S. Geol. Surv. Open File Rep., 96–669*, 30 pp.

Raymo, M. E., W. F. Ruddiman, and B. M. Clement (1987), Pliocene-Pleistocene paleoceanography of the North Atlantic at Deep Sea Drilling Project Site 609, *Initial Rep. Deep Sea Drill. Proj.*, *94*, 895–901.

Reynolds, R. W., and T. M. Smith (1995), A high resolution global sea surface temperature climatology, *J. Clim.*, *8*, 1571–1583, doi:10.1175/1520-0442(1995)008<1571:AHRGSS>2.0.CO;2.

Savin, S. M., L. Abel, E. Barrera, D. Hodell, J. P. Kennett, M. Murphy, G. Keller, J. Killingley, and E. Vincent (1985), The evolution of Miocene surface and near-surface marine temperatures: Oxygen isotopic evidence, in *The Miocene Ocean*, edited by J. P. Kennett, *Mem. Geol. Soc. Am.*, *163*, 49–82.

Schiebel, R., J. Bijma, and C. Hemleben (1997), Population dynamics of the planktic foraminifer Globigerina bulloides from the eastern North Atlantic, *Deep Sea Res., Part I*, *44*, 1701–1713, doi:10.1016/S0967-0637(97)00036-8.

Shackleton, N. J., M. A. Hall, and D. Pate (1995), Pliocene stable isotope stratigraphy of Site 846, *Proc. Ocean Drill. Program Sci. Results*, *138*, 337–355.

Sloan, L. C., T. J. Crowley, and D. Pollard (1996), Modeling of middle Pliocene climate with the NCAR GENESIS general circulation model, *Mar. Micropaleontol.*, *27*, 51–61, doi:10.1016/0377-8398(95)00063-1.

Thierstein, H. R., K. R. Geitzenauer, B. Molfino, and N. Shackleton (1977), Global synchroneity of late Quaternary coccolith datum levels: Validation by oxygen isotopes, *Geology*, *5*, 400–404, doi:10.1130/0091-7613(1977)5<400:GSOLQC>2.0.CO;2.

Willard, D. A. (1994), Palynological record from the North Atlantic region at 3 Ma: Vegetational distribution during a period of global warmth, *Rev. Palaeobot. Palynol.*, *83*, 275–297, doi:10.1016/0034-6667(94)90141-4.

H. J. Dowsett and M. M. Robinson, U.S. Geological Survey, 926A National Center, Reston, VA 20192, USA. (mmrobinson@usgs.gov)

G. S. Dwyer, Division of Earth and Ocean Sciences, Nicholas School of the Environment and Earth Sciences, Duke University, Durham, NC 27708, USA.

K. T. Lawrence, Geology and Environmental Geosciences, Lafayette College, Easton, PA 18042, USA.